

Supporting Information for Subramanian et al.

Supplementary Figure legends

Supplementary Figure 1: G-quadruplex structures are present in the 3'-end of PSD-95 and CaMKIIa mRNA 3'-UTRs **A**, Reverse transcriptase (RT) elongation of ³²P-radiolabelled primers hybridized onto PSD-95 (human) and CaMKIIa (rat) 3'-UTR RNA transcripts shows the presence of strong potassium-dependent RT stops at the 3'-end of a Gq forming sequence. In presence of 150 mM KCl, most of RT elongation is stopped at position 717 and 3059 in PSD-95 and CaMKIIa 3'-UTRs, respectively (lanes K), while elongations proceed to the 5'-end of RNAs in presence of 150 mM LiCl (lanes Li). Secondary structure model of the Gqs motives in PSD-95 and CaMKIIa mRNAs is presented (numbering from first nucleotide of 3'-UTR). **B**, Guanines in the Gq forming regions of PSD-95 and CaMKIIa RNAs exhibit RNase T1 protections in 150 mM KCl (K) compared to 150 mM LiCl (Li). Experiment shown is a RT as in Figure 1A, with RNA transcripts treated with RNase T1 (+) or untreated (-). T1 cuts are indicated by arrows. T1 protections (-) and increases of reactivity (+) are indicated. **C**, Example of autoradiographs presenting the reactivity of PSD95 3'-UTR RNA towards V1, T1, DMS and CMCT. Lanes C are controls without enzyme or reagent. Lanes 1 and 2 are 5 and 10 min incubation time with the indicated reagent respectively.

Supplementary Figure 2: Alignments of the G-quadruplex forming sequence of PSD95 and CaMKIIa 3'-UTRs from mammals.

Supplementary Figure 3: The lambda-GFP RNA reporter system from (Daigle & Ellenberg, 2007) enables the efficient visualization of a reporter mRNA bearing the β -actin zipcode in the neurites of live cortical neurons. **A**, transfection of RNA reporter plasmid lacking boxB (pmRFP- β -actin-zipcode) and fluorescent-reporter p4lambda-N22-3mEGFP-M9). The fluorescent-reporter cannot interact with the BoxB-less RNA, thus it stays in nucleus because of its M9 nuclear localization signal. Red fluorescent protein diffuses throughout cytoplasm. **B**, transfection of pmRFP-4boxB- β -actin-zipcode and fluorescent-reporter p4lambda-N22-3mEGFP-M9. The fluorescent-reporter interacts with mRNA reporter, is exported from the nucleus, and is efficiently localized in dendrites. **C**, transfection of pmRFP-4boxB and fluorescent-reporter p4lambda-N22-3mEGFP-M9. The fluorescent-reporter interacts with mRNA reporter, is exported from the nucleus but is poorly localized in dendrites. E17 mouse cortical neurons were transfected at 7 DIV and imaged 10h later. Contrast has been adjusted equally between figures for display purposes. Images are projections of 10 fluorescence confocal sections of 1.5 μ m. Scale bar, 15 μ m.

Supplementary Figure 4: Visualization of PSD95 and CaMKIIa 3'-UTRs-containing reporter mRNAs in cortical neurons with fluorescent *in situ* hybridization using a multilabelled Alexa-488 oligodesoxynucleotide probe (green). Cells were treated as in Figure 2 but without using p4lambda-N22-3mEGFP-M9. Scale bar, 20 μ m.

Supplementary Figure 5: The deletion of the G-quadruplex elements in PSD95 and CaMKIIa 3'-UTR mRNAs has no apparent impact on RNA stability, translation efficiency and poly-A tail length. **A**, Levels of reporter mRNAs with PSD95, PSD95- Δ G, CaMKIIa and CaMKIIa Δ G 3'-UTRs determined by qRT-PCR in cortical neurons. Neurons were transfected with the RNA-reporter expression plasmids (pDsRBB-variants) as in Figure 2. Data are the mean results with standard deviation of three independent transfection experiments with qPCR performed in triplicates for each). Actinomycin D treatment (10 μ g.ml⁻¹) of the neurons

2 and 6h prior RNA extraction did not significantly change the RNA levels between PSD95 and PSD95-ΔG, CaMKIIa and CaMKIIaΔG. **B**, The length of the poly-A tail of reporter mRNAs with PSD95, PSD95-ΔG, CaMKIIa and CaMKIIaΔG 3'-UTRs in cortical neurons was not found different as determined by radioactive PCR as in (Murray & Schoenberg, 2008). **C**, control with A20 oligodeoxynucleotide, N1 and N3 are “no-RT” controls with 2 μg total RNA extracted from pDsRBB-PSD95 and pDsRBB-CaMKIIa transfected cortical neurons, respectively, “0” is control with RNA extracted from non transfected neurons, 1, 2, 3, 4 are assays with 2 μg total RNA extracted from pDsRBB-PSD95-812, pDsRBB-PSD95-812Δ, pDsRBB-CaMKIIa-3112 and pDsRBB-CaMKIIa-3112ΔG transfected cortical neurons, respectively. Details of the polyA tail length measure are given in supplementary method section. **C**, Luciferase reporter expression assay performed on extracts of cortical neurons transfected with plasmid pRLTK bearing PSD95-812, PSD95-812ΔG, CaMKIIa-3112, or CaMKIIa-3112ΔG sequences cloned into *Xba*I site and plasmid pFluc. Results are the ratio of Renilla luciferase activity/Firefly luciferase activity x100. Data are the mean results with standard deviation of three independent transfection experiments with luciferase assays performed in triplicate for each.

Supplementary Figure 6: Sequence of variable region in 3'-UTR of pDsRBB-“variants” RNA transcripts. The stops of reverse transcription observed in Fig. 3C are indicated by arrows.

Supplementary Figure 7: PSD95 and CaMKIIa 3'-UTR RNAs are bound specifically by FMRP *via* the G-quadruplex structure *in vitro* and FMRP contributes to DHPG enhanced localization of CaMKIIa 3'-UTR-bearing reporter. **A**, Competition experiments to determine the binding specificity of FMRP for PSD-95 and CaMKIIa 3'-UTRs by gel retardation. ³²P-labeled N19 subfragment of FMR1 mRNA (the 425 nt-long canonical FMRP binding site (Schaeffer et al, 2001)) containing a G-quadruplex was incubated with recombinant GST-FMRP (0.1 pmol) in the presence of the indicated increasing amounts of unlabelled competitors ((i) PSD95-812, PSD95ΔG-812 (ii) CaMKIIa-3112, CaMKIIaΔG-3112). The graph depicts the fraction of bound labeled N19 RNA plotted against unlabeled competitor RNA concentration. Each point is the mean with standard deviation of at least three independent experiments. **B**, Cation dependent binding of FMRP with PSD95-219 and CaMKIIa-263 3'-UTRs. Importantly, these shorter RNA fragments had the same efficiency of FMRP binding as the full length 3'-UTRs (as tested by the competition assay presented in A), the same efficiency of RT arrest with KCl and the same NTE efficiency (data not shown). Labeled PSD95-219 and CaMKIIa-263 RNA transcripts were incubated with the indicated amounts (pmol) of GST-FMRP in presence of binding buffer containing 150 mM of KCl or LiCl. The bound RNAs (determined by phosphorimager quantification) were plotted against the amount of GST-FMRP. Each point is the mean with standard deviation of at least three independent experiments. **C**, Influence of the absence of FMRP on the localization of PSD-95 or CaMKIIa 3'-UTR-bearing reporter mRNAs in neurites of cortical neurons. Neurons from *FMRI* wild type (Wt) or null (KO) mice were treated and imaged as in Fig. 3B. Mean values of mRNA reporter localization with standard deviations for cell bodies and various distances within dendrites were calculated per constructs or genotype and are shown as arbitrary fluorescence units. Statistical significance was established using paired Student's T test. *, $p < 0.05$ for CaMKIIa stimulated *FMRI* KO versus *FMRI* Wt. Although PSD95 3'-UTR-bearing reporter mRNA showed a trend of reduced neuritic localization in KO versus Wt, the differences between replicates were not statistically significant.

Supplementary Movie 1: Fast movement of PSD-95 3'UTR RNA reporter in cortical neuron visualized with the lambda-GFP system. Time-lapse confocal (spinning disk) analysis with total recording time of 1 min 20 sec, 1 frame/sec with each frame being 500 ms recording time.

Supplementary Materials and Methods

Ethics statement

Animal work involved in this study was conducted according to relevant national CNREEA (Comité National de Réflexion Ethique en Expérimentation Animale) and international guidelines (86/609/CEE).

Plasmid constructs

pDsRed-Mono-4BB: RNA-reporter expression vector; sense and antisense oligonucleotides (GGCCAGCCCTGAAAAAGGGCTCGAGCCCTGAAAAAGGGCAATTGCCCTGAAAAAGGGCGTCGACGCCCTGAAAAAGGGC, GGCCGCCCTTTTTTCAGGGCGTCGACGCCCTTTTTTCAGGGCAATTGCCCTTTTTTCAGGGCTCGAGCCCTTTTTTCAGGGCT, respectively) containing four boxB flanked by *NotI* restriction sites were annealed, kinase treated, and ligated into *NotI* site of pDsred-monomer-N1 vector (Clontech) to create pDsRed-Mono-4BB.

pDsRBB-PSD95-812 : The 3'UTR of PSD-95 (812nt) was cloned by PCR from human placental DNA using TA-Topocloning (Invitrogen), DNA fragment corresponding to 3'UTR was then sequence verified and cloned into *XbaI* site pDsRed-Mono-4BB to give pDsRBB-PSD95-812 using following primers: forward 5'-ACGTCTAGATTCCTGCCCTGGCTTGGCCTG, reverse 5'-TGCTCTAGACTGTCTCTTCCTTCACTCTCTC.

pDsRBB-CaMKIIa-3112 : The 3'UTR of CaMKIIa was PCR cloned from vector containing the 3'UTR of CaMKIIa (3112 nt-Rat) (Mori et al, 2000) into *XbaI* site of pDsRed-M-4BB to give pDsRBB-CaMKIIa-3112 using following primers: forward 5'-ACGTCTAGACTTCTTTGTTACTACTTGTTTAG, reverse 5'-TGCTCTAGAAAATTTGTAGCTATTTATTCCACTG.

pDsRBB-PSD95-812 Δ G and pDsRBB-CaMKIIa-3112 Δ G were constructed by deleting the G-quadruplex forming sequence from the pDsRBB-PSD95-812 and pDsRBB-CaMKIIa-3112 construct using oligonucleotides (sense TGGGTCTAGGGAGTGGGAAATGCTGTCCGGGAGCCAGGGAAAGACTGGA, antisense TCCAGTCTTCCCTGGCTCCCGGACAGCATTTCCTCCACTCCCTAGACCCA) and (sense CCATTGCTCAAACCTTTCTGCTAAGAAGACGTCTGTTTTATTCTTGG, antisense CCAAGAATAAAACAGACGTCTTCTTAGCAGAAAGTTTGAGCAATGG). PSD-Gq, CaMKIIa-Gq, non-Gq, G-rich, Gq(A), Gq(T), Gq3 and Gq2 were either PCR amplified or oligo annealed with respective primers and cloned into *XbaI* site of pDsred-M-4BB vector.

PSD-Gq Forward Reverse	CATCTAGAAGTGGAAGGTCTAAATGTGGC CATCTAGACAAGTACTGTCTCTTCCTTTC
CaMKIIa-Gq Sense Antisense	CTAGGGGGGGTGGGTGGGGGAGGGGAGAAGAGA CTAGTCTCTTCTCCCTCCCCACCCACCCCCC
Non-Gq Sense Antisense	CTAGGGAAGAGGAGAGGAGGGA CTAGTCCCTCCTCTCCTCTTCC

G-rich Sense Antisense	CTAGGGGAGGGGAGGGG CTAGCCCCACCCACCC
Gq(A) Sense Antisense	CTAGGGGAGGGGAGGGGAGGGG CTAGCCCCTCCCCTCCCCTCCC
Gq(T) Sense Antisense	CTAGGGGTGGGGTGGGGTGGGG CTAGCCCCACCCACCCACCC
Gq3 Sense Antisense	CTAGGGAAGGGAAGGGAAGGG CTAGCCCTTCCCTTCCCTTCC
Gq2 Sense Antisense	CTAGGAAGGAAGGAAGG CTAGCCTTCCTTCCTTC

Chemical and Enzymatic probing

RNA structure probing was performed as in Moine et al, (1998). Briefly, 5 pmol of T7 RNA transcripts of PSD95-812 and CaMKIIa-3112 3'-UTR RNAs were renatured 15 min at 40° C in 19 µl native buffer (50 mM Hepes buffer pH 7.5 for DMS (dimethyl sulfate), or 50 mM borate buffer pH 8.0 for CMCT (1-cyclohexyl-(2-morpholinoethyl)carbodiimide metho-p-toluene sulfonate), 5 mM MgCl₂, 75 mM KCl, 5 mM EDTA, 2 µg tRNA). Modifications were performed using 1 µl of either DMS (1:2 v/v in ethanol) or CMCT (60 µg) at 20° C for 5 and 15 min, respectively. Enzymatic modifications were performed with RNase T1 (0.05 U and 0.1 U) and RNase V1 (0.05 U and 0.1 U) for 5 min at 20° C, followed by phenol/chloroform extraction. After ethanol precipitation and solubilization in appropriate buffer, RNAs were reverse-transcribed and analyzed on gel as previously described (Schaeffer et al, 2001).

Luciferase constructs

pRLTK-PSD95-812, pRLTK-PSD95-812ΔG, pRLTK-CaMKIIa-3112 and pRLTK-CaMKIIa-3112ΔG were constructed by PCR amplification and ligation into the *Xba*I site of pRLTK vector (Promega) using the following primers for PSD-95 forward GAGAGAGACTCTGATTCCT, reverse CAAGTATCTGTCTCTTCCT whereas CaMKIIa primers were the same as above.

Luciferase activity assays

Primary cortical neurons were transfected in triplicates in 24-well plates at 7 DIV with pRLTK-PSD95-812 or pRLTK-CaMKIIa-3112, vectors expressing *Renilla* luciferase (Promega) with the full length PSD-95 and CaMKIIa 3'-UTR inserted in *Xba*I site and pFlashSV40 plasmid (Synsys), expressing *Firefly* luciferase and used as normalizer. Luciferase activities were measured 24 hours later with Dual Luciferase Assay System (Promega) according to manufacturer instructions.

Real-time reverse transcriptase PCR

Total RNAs from primary cortical neurons transfected with plasmids pRLTK or pDsRBB (-PSD95-812, -PSD95-812ΔG, -CaMKIIa-3112 or -CaMKIIa-3112ΔG) were extracted using RNeasy Mini Kit (Qiagen) as described by the manufacturer. Reverse transcription reactions were performed on 2 µg of total RNA with gene specific primers by using SuperScriptTM II (Invitrogen) as described by the manufacturer. Quantification of relative amounts of mRNA

were calculated using the $\Delta\Delta CT$ method. Real time PCR were performed on 1/100 dilution of each sample in triplicate with QuantiTect SYBR Green PCR Kits (Qiagen) in a Light cycler 480 real-time PCR system (Roche diagnostics). The real-time PCR reactions were carried out in the presence of 10 pmol of reverse and forward gene specific primers:

Oligos Renilla

forward 5'-GTAAAAGGTGGTAAACCTG

reverse 5'-GACAAATTCAGTATTAGGAAAC

Oligos Firefly

forward 5'-TTCCATCTTCCAGGGATACG

reverse 5'-ATCCAGATCCACAACCTTCG

Oligos DsRed

forward 5'-CTCCACCGAGAAGCTGTACC

reverse 5'-CTCCACCACGGTGTAGTCCT

PolyA tail length measure assay

The length of polyA tail of RNAs expressed from pDsRBB-PSD95-812, pDsrRBB-PSD95-812 Δ G, pDsRBB-CaMKIIa-3112 and pDsRBB-CaMKIIa-3112 Δ G was assayed according to Murray & Schoenberg (2008) with the following modifications: total RNA was Trizol extracted from three 24-well transfected (as described in Material and Methods) cortical neuron cultures and was isopropanol precipitated in presence of 0.5 μ g of glycogen and treated with RNase free DNase. RNA was phenol/choroform extracted, reprecipitated by ethanol and resuspended in 10 μ l mQ H₂O. cDNA synthesis was performed with 300 ng oligonucleotide adapter "polyA" annealed on 2 μ g total RNA (5 min 85°C, 5 min 0°C) or on 300 ng oligonucleotide "control polyA20" in 20 μ l reaction volume using Superscript II (Invitrogen) following manufacturer instructions. Radioactive PCR was performed on 3 μ l of the cDNA mix in presence of 30,000 cpm (Cerenkov) of 5'-end 32P labelled "polyAtail-forward" primer, 2 min at 95°C, and 25 cycles with 0.5 min at 94°C, 0.5 min at 60°C, 0.5 min at 72°C. PCR product was visualized on 6 % PAGE with 8 M urea.

- Oligo adapter polyA (reverse)

GGGGATCCGCGGTTTTTTTTTTT

- Oligo control polyA20

GAATGCAATTGTTGTTGaaaaaaaaaaaaaaaaaaaa

- Oligos polyAtail-forward

GAATGCAATTGTTGTTG

Imaging and quantification

Fluorescence intensity of equally sized areas in cell bodies and in their dendrites at various distances from cell bodies was measured on pictures taken with the same settings using 63x objective with a Leica DMRXA2 microscope equipped with EMCCD Roper Cascade 2 camera and operated with Metamorph. Fluorescence was measured by tracing a defined region of interest (ROI) and the fluorescence normalized for area (ImageJ NIH). Dendrites segments (3 per neuron) were taken at 20, 40, 80 μ m away from the cell body. Background (normalized for area) from regions on the coverslips outside the cell was subtracted from each dendritic measurement to attain an average dendritic intensity. For Lambda-GFP system results are expressed as percentage of cells showing a dendritic localization: presence of GFP signal along the dendrites (i.e in three segments) among those expressing the fluorescent-reporter. For FISH experiments and measure of DHPG effect, mean values with standard deviations for dendritic localization were calculated per constructs and shown as arbitrary fluorescence unit (AFU). Statistical significance was established using paired Student's t test.

Data were derived from at least three different transfections per construct tested and with neurons originating from three mice per genotype.

Supplementary Tables

Table 1: Short list of best reported dendritic RNAs and presence of G-quadruplex ($G_{\geq 3}N_{0-6}$)₄ in their 3'-UTR.

Gene	Technique (location : c(cortex), h(hippocampus) dg (dentate gyrus), s(striatum), SN(synaptoneuroosomes))	Localisation element	comments	G- quadruplex prediction in 3'UTR ^a	G-quadruplex sequence	Reference ^b
<u>β-actin</u> <u>NM_001101.3</u>	FISH	54 nt Zipcode (3'UTR)		-		(1)
<u>APP</u> <u>NM_000484.3</u>	RT-PCR SN			+	<u>GGGGCGGGTGGGGAG</u> <u>GGG</u>	(2)
<u>Arc (arg3.1)</u> <u>NM_015193.3</u>	FISH (c,h,dg) Radioactive ISH (c, h)	350 nt (3'UTR)		-		(3-5)
<u>BDNF</u> <u>NM_170735.5</u>	FISH	(3'UTR)		+	<u>GGGGATGGGGATGG</u> <u>GGGG</u>	(6,7)
<u>Calmodulin</u> <u>NM_006888.4</u>	FISH (c,h,purkinje)			-		(8)
<u>α-CaMKII</u> <u>NM_015981.2</u>	FISH (c,h,dg)	- 1200 nt, 30 nt (αCaMKII/Ng dendritic localization element, CNDLE) - CPE	KCL, DHPG activated (FMRP- dependent)	+	<u>GGGGGGCGGGTGGG</u> <u>ATGGGAAGAAGGGG</u>	(9-12)
<u>CREB</u> <u>NM_004379.3</u>	Radioactive ISH (hippocampal neurons)			-		(13)
<u>Dendrin</u> <u>NM_015086.1</u>	FISH (c,h,dg)	1000 nt (3'UTR)		+	<u>GGAGGGCAGGGTAGG</u> <u>GTAGGG</u>	(14,15)
<u>FMRP</u> <u>NM_002024.5</u>	RT-PCR			-		(16)
<u>G protein gamma 7 sub.</u> <u>NM_052847.2</u>	FISH (c,h,dg,s)			+	<u>GGGAGGGCTGGGGCT</u> <u>TCGGG</u>	(17)
<u>GABA-A-R-g</u> <u>NM_001470.2</u>	FISH (cortical neurons)		DHPG activated (FMRP- dependent)	-		(11)
<u>Glycine receptor (GLRA1)</u> <u>NM_000171.3</u>	FISH (motoneuron)			+	<u>GGGGGAGGCTGGGAG</u> <u>AGGGGAACGTGGG</u>	(18)
<u>InsP3R1</u> <u>NM_001099952.2</u>	FISH Purkinje cells			-		(19)
<u>Ligatin</u> <u>NM_006893.2</u>	FISH			-		(20)
<u>MAP1b</u> <u>NM_005909.3</u>	FISH (cortical neurons)		DHPG activated (FMRP- dependent)	-		(11)
<u>MAP2</u> <u>NM_002374.3</u>	FISH (c,h,dg)	640 nt (3'UTR)		-		(21-24)

MRG15 (MORF4L1) <u>NM_006791.2</u>	FISH widespread			-		(25)
Neurogranin <u>NM_001126181.1</u>	ISH histochemistry	30 nt (3'UTR) α CaMKII/Ng dendritic localization element (CNDLE)		-		(12,26)
Neurofilament protein 68 <u>NM_006158.3</u>	FISH Vestibular neurons			-		(27)
NEURL <u>NM_004210.4</u>	FISH widespread			+	<u>GGGATGGGCCAGGGC</u> <u>CCTGGGTGGG</u>	(28)
NMDAR1 <u>NM_000832.6</u>	FISH (dg)	(5'UTR)		-		(29)
Pcp2(L7) <u>NM_001129804.1</u>	FISH Purkinje cells	65 nt (3'UTR)		-		(30,31)
PEP19 <u>NM_006198.2</u>	FISH Purkinje cells			-		(19)
PSD95 (DLG4) <u>NM_001365.3</u>	RT-PCR			+	<u>GGGGAAAAGGGAGGG</u> <u>ATGGGTCTAGGGAGT</u> <u>GGGAAATGCGGGAGG</u> <u>GAGGGTGGGGGCAG</u> <u>GGGTCGGG</u>	(32)
RGS5 <u>NM_003617.3</u>	FISH (cortical neurons)			-		(11)
SAPAP4 (DLGAP4) <u>NM_001042486.2</u>	FISH (cortical neurons)		DHPG activated (FMRP- dependent)	+	<u>GGGCGGGGTAGGGGA</u> <u>GGGCAGGGG</u>	(11)
Shank1 AY461452	FISH widespread	200 nt (3'UTR)		+	<u>GGGAGGGTCACGGGA</u> <u>GGGGGGAGGGG...GGG</u> <u>GTTGGGGAGGGTGTA</u> <u>GGGGGTGGGGGTGGG</u> <u>GGTGAAGGAGAGGG</u> <u>GAGAGGGAAGGGGGA</u> <u>GGG</u>	(33,34)
Shank3 <u>NM_001080420.1</u>	FISH widespread			+	<u>GGGCGGGAGGTGCC</u> <u>GGGGGTGGGG...GGGG</u> <u>GGAGGGGGGAGACAT</u> <u>TGGG...GGGGTGGGGG</u> <u>GCCC TGGG</u>	(34)
TrkB <u>NM_001007097.1</u>	FISH			-		(35)
Vasopressin (AVP) <u>NM_000490.4</u> oxytocin (OXT) <u>NM_000915.2</u>	FISH (hypothalamo- hypophysial)	(ORF +3'UTR)		-		(36,37)
BC1	Radioactive ISH	GA kink-turn (KT) motif		-		(38,39)
ribosomal RNAs	Radioactive ISH			-		(40)
tRNAs	Radioactive ISH			-		(41)

^aprediction of G-quadruplex consensus ($G_{\geq 3}N_{1-6}$)₄ using QGRS-mapper (<http://bioinformatics.ramapo.edu/QGRS/>) (42) and visual inspection and conserved between human and rodents.

^bReferences :

1. Zhang, H.L., Eom, T., Oleynikov, Y., Shenoy, S.M., Liebelt, D.A., Dichtenberg, J.B., Singer, R.H. and Bassell, G.J. (2001) Neurotrophin-induced transport of a beta-actin mRNP complex increases beta-actin levels and stimulates growth cone motility. *Neuron*, **31**, 261-275.
2. Westmark, C.J. and Malter, J.S. (2007) FMRP mediates mGluR5-dependent translation of amyloid precursor protein. *PLoS Biol*, **5**, e52.
3. Lyford, G.L., Yamagata, K., Kaufmann, W.E., Barnes, C.A., Sanders, L.K., Copeland, N.G., Gilbert, D.J., Jenkins, N.A., Lanahan, A.A. and Worley, P.F. (1995) Arc, a growth factor and activity-regulated gene, encodes a novel cytoskeleton-associated protein that is enriched in neuronal dendrites. *Neuron*, **14**, 433-445.
4. Link, W., Konietzko, U., Kauselmann, G., Krug, M., Schwanke, B., Frey, U. and Kuhl, D. (1995) Somatodendritic expression of an immediate early gene is regulated by synaptic activity. *Proc Natl Acad Sci U S A*, **92**, 5734-5738.
5. Kobayashi, H., Yamamoto, S., Maruo, T. and Murakami, F. (2005) Identification of a cis-acting element required for dendritic targeting of activity-regulated cytoskeleton-associated protein mRNA. *Eur J Neurosci*, **22**, 2977-2984.
6. Tongiorgi, E., Armellini, M., Giulianini, P.G., Bregola, G., Zucchini, S., Paradiso, B., Steward, O., Cattaneo, A. and Simonato, M. (2004) Brain-derived neurotrophic factor mRNA and protein are targeted to discrete dendritic laminae by events that trigger epileptogenesis. *J Neurosci*, **24**, 6842-6852.
7. An, J.J., Gharami, K., Liao, G.Y., Woo, N.H., Lau, A.G., Vanevski, F., Torre, E.R., Jones, K.R., Feng, Y., Lu, B. *et al.* (2008) Distinct role of long 3' UTR BDNF mRNA in spine morphology and synaptic plasticity in hippocampal neurons. *Cell*, **134**, 175-187.
8. Berry, F.B. and Brown, I.R. (1996) CaM I mRNA is localized to apical dendrites during postnatal development of neurons in the rat brain. *J Neurosci Res*, **43**, 565-575.
9. Burgin, K.E., Waxham, M.N., Rickling, S., Westgate, S.A., Mobley, W.C. and Kelly, P.T. (1990) In situ hybridization histochemistry of Ca²⁺/calmodulin-dependent protein kinase in developing rat brain. *J Neurosci*, **10**, 1788-1798.
10. Huang, Y.S., Carson, J.H., Barbarese, E. and Richter, J.D. (2003) Facilitation of dendritic mRNA transport by CPEB. *Genes Dev*, **17**, 638-653.
11. Dichtenberg, J.B., Swanger, S.A., Antar, L.N., Singer, R.H. and Bassell, G.J. (2008) A direct role for FMRP in activity-dependent dendritic mRNA transport links filopodial-spine morphogenesis to fragile X syndrome. *Dev Cell*, **14**, 926-939.
12. Mori, Y., Imaizumi, K., Katayama, T., Yoneda, T. and Tohyama, M. (2000) Two cis-acting elements in the 3' untranslated region of alpha-CaMKII regulate its dendritic targeting. *Nat Neurosci*, **3**, 1079-1084.
13. Crino, P., Khodakhah, K., Becker, K., Ginsberg, S., Hemby, S. and Eberwine, J. (1998) Presence and phosphorylation of transcription factors in developing dendrites. *Proc Natl Acad Sci U S A*, **95**, 2313-2318.
14. Herb, A., Wisden, W., Catania, M.V., Marechal, D., Dresse, A. and Seeburg, P.H. (1997) Prominent dendritic localization in forebrain neurons of a novel mRNA and its product, dendrin. *Mol Cell Neurosci*, **8**, 367-374.
15. Kremerskothen, J., Kindler, S., Finger, I., Veltel, S. and Barnekow, A. (2006) Postsynaptic recruitment of Dendrin depends on both dendritic mRNA transport and synaptic anchoring. *J Neurochem*, **96**, 1659-1666.
16. Zalfa, F., Eleuteri, B., Dickson, K.S., Mercaldo, V., De Rubeis, S., di Penta, A., Tabolacci, E., Chiurazzi, P., Neri, G., Grant, S.G. *et al.* (2007) A new function for the fragile X mental retardation protein in regulation of PSD-95 mRNA stability. *Nat Neurosci*, **10**, 578-587.
17. Watson, J.B., Coulter, P.M., 2nd, Margulies, J.E., de Lecea, L., Danielson, P.E., Erlander, M.G. and Sutcliffe, J.G. (1994) G-protein gamma 7 subunit is selectively expressed in medium-sized neurons and dendrites of the rat neostriatum. *J Neurosci Res*, **39**, 108-116.
18. Racca, C., Gardiol, A. and Triller, A. (1997) Dendritic and postsynaptic localizations of glycine receptor alpha subunit mRNAs. *J Neurosci*, **17**, 1691-1700.
19. Furuichi, T., Simon-Chazottes, D., Fujino, I., Yamada, N., Hasegawa, M., Miyawaki, A., Yoshikawa, S., Guenet, J.L. and Mikoshiba, K. (1993) Widespread expression of inositol 1,4,5-trisphosphate receptor type 1 gene (Insp3r1) in the mouse central nervous system. *Receptors Channels*, **1**, 11-24.
20. Severt, W.L., Biber, T.U., Wu, X., Hecht, N.B., DeLorenzo, R.J. and Jakoi, E.R. (1999) The suppression of testis-brain RNA binding protein and kinesin heavy chain disrupts mRNA sorting in dendrites. *J Cell Sci*, **112 (Pt 21)**, 3691-3702.
21. Garner, C.C., Tucker, R.P. and Matus, A. (1988) Selective localization of messenger RNA for cytoskeletal protein MAP2 in dendrites. *Nature*, **336**, 674-677.
22. Bruckenstein, D.A., Lein, P.J., Higgins, D. and Fremeau, R.T., Jr. (1990) Distinct spatial localization of specific mRNAs in cultured sympathetic neurons. *Neuron*, **5**, 809-819.

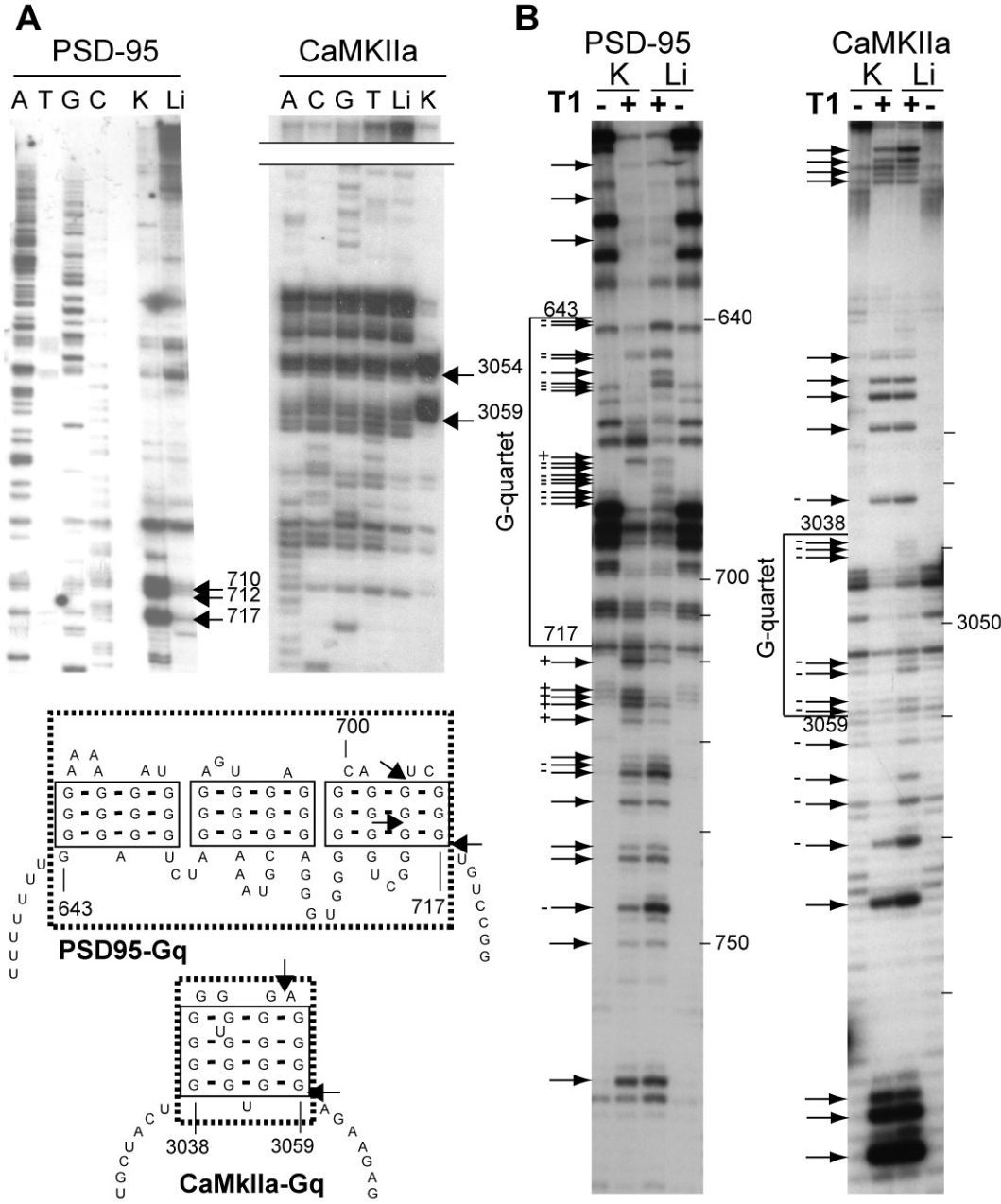
23. Kleiman, R., Banker, G. and Steward, O. (1990) Differential subcellular localization of particular mRNAs in hippocampal neurons in culture. *Neuron*, **5**, 821-830.
24. Blichenberg, A., Schwanke, B., Rehbein, M., Garner, C.C., Richter, D. and Kindler, S. (1999) Identification of a cis-acting dendritic targeting element in MAP2 mRNAs. *J Neurosci*, **19**, 8818-8829.
25. Matsuoka, Y., Shibata, S., Ban, T., Toratani, N., Shigekawa, M., Ishida, H. and Yoneda, Y. (2002) A chromodomain-containing nuclear protein, MRG15 is expressed as a novel type of dendritic mRNA in neurons. *Neurosci Res*, **42**, 299-308.
26. Landry, C.F., Watson, J.B., Kashima, T. and Campagnoni, A.T. (1994) Cellular influences on RNA sorting in neurons and glia: an in situ hybridization histochemical study. *Brain Res Mol Brain Res*, **27**, 1-11.
27. Paradies, M.A. and Steward, O. (1997) Multiple subcellular mRNA distribution patterns in neurons: a nonisotopic in situ hybridization analysis. *J Neurobiol*, **33**, 473-493.
28. Timmusk, T., Palm, K., Belluardo, N., Mudo, G. and Neuman, T. (2002) Dendritic localization of mammalian neuralized mRNA encoding a protein with transcription repression activities. *Mol Cell Neurosci*, **20**, 649-668.
29. Benson, D.L. (1997) Dendritic compartmentation of NMDA receptor mRNA in cultured hippocampal neurons. *Neuroreport*, **8**, 823-828.
30. Zhang, R., Zhang, X., Bian, F., Pu, X.A., Schilling, K. and Oberdick, J. (2008) 3'UTR-dependent localization of a Purkinje cell messenger RNA in dendrites. *Cerebellum*, **7**, 482-493.
31. Bian, F., Chu, T., Schilling, K. and Oberdick, J. (1996) Differential mRNA transport and the regulation of protein synthesis: selective sensitivity of Purkinje cell dendritic mRNAs to translational inhibition. *Mol Cell Neurosci*, **7**, 116-133.
32. Muddashetty, R.S., Kelic, S., Gross, C., Xu, M. and Bassell, G.J. (2007) Dysregulated metabotropic glutamate receptor-dependent translation of AMPA receptor and postsynaptic density-95 mRNAs at synapses in a mouse model of fragile X syndrome. *J Neurosci*, **27**, 5338-5348.
33. Falley, K., Schutt, J., Iglauer, P., Menke, K., Maas, C., Kneussel, M., Kindler, S., Wouters, F.S., Richter, D. and Kreienkamp, H.J. (2009) Shank1 mRNA: dendritic transport by kinesin and translational control by the 5'untranslated region. *Traffic*, **10**, 844-857.
34. Bockers, T.M., Segger-Junius, M., Iglauer, P., Bockmann, J., Gundelfinger, E.D., Kreutz, M.R., Richter, D., Kindler, S. and Kreienkamp, H.J. (2004) Differential expression and dendritic transcript localization of Shank family members: identification of a dendritic targeting element in the 3' untranslated region of Shank1 mRNA. *Mol Cell Neurosci*, **26**, 182-190.
35. Tongiorgi, E., Righi, M. and Cattaneo, A. (1997) Activity-dependent dendritic targeting of BDNF and TrkB mRNAs in hippocampal neurons. *J Neurosci*, **17**, 9492-9505.
36. Mohr, E., Meyerhof, W. and Richter, D. (1995) Vasopressin and oxytocin: molecular biology and evolution of the peptide hormones and their receptors. *Vitam Horm*, **51**, 235-266.
37. Prakash, N., Fehr, S., Mohr, E. and Richter, D. (1997) Dendritic localization of rat vasopressin mRNA: ultrastructural analysis and mapping of targeting elements. *Eur J Neurosci*, **9**, 523-532.
38. Tiedge, H., Freneau, R.T., Jr., Weinstock, P.H., Arancio, O. and Brosius, J. (1991) Dendritic location of neural BC1 RNA. *Proc Natl Acad Sci U S A*, **88**, 2093-2097.
39. Muslimov, I.A., Iacoangeli, A., Brosius, J. and Tiedge, H. (2006) Spatial codes in dendritic BC1 RNA. *J Cell Biol*, **175**, 427-439.
40. Kleiman, R., Banker, G. and Steward, O. (1993) Subcellular distribution of rRNA and poly(A) RNA in hippocampal neurons in culture. *Brain Res Mol Brain Res*, **20**, 305-312.
41. Tiedge, H. and Brosius, J. (1996) Translational machinery in dendrites of hippocampal neurons in culture. *J Neurosci*, **16**, 7171-7181.
42. Kikin, O., Zappala, Z., D'Antonio, L. and Bagga, P.S. (2008) GRSDDB2 and GRS_UTRdb: databases of quadruplex forming G-rich sequences in pre-mRNAs and mRNAs. *Nucleic Acids Res*, **36**, D141-148.

Supplementary table 2: List of 500 randomly chosen mRNAs and presence of G-quadruplex in their 3'-UTR.

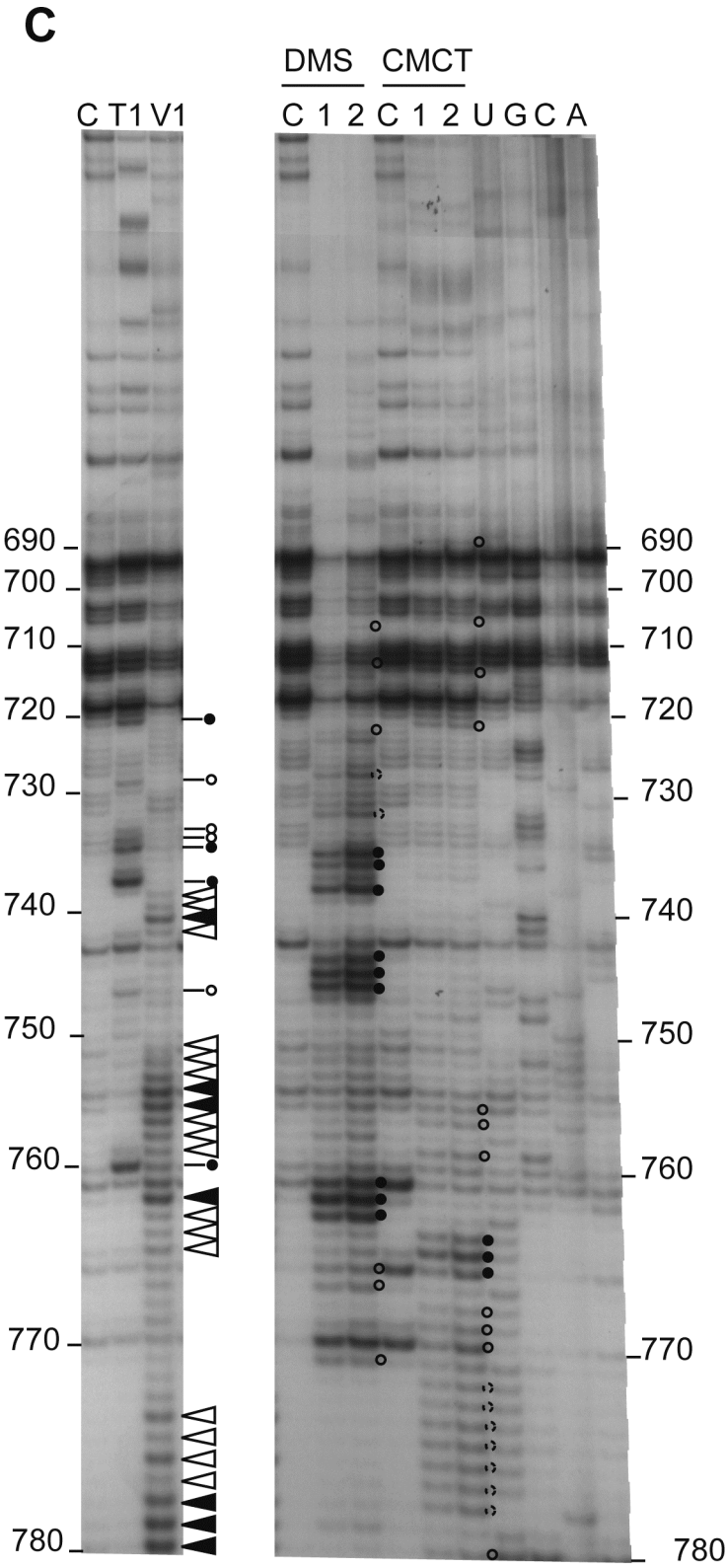
(please see .xls file in supplementary information)

Supplementary Figures

Supplementary Figure S1AB



Supplementary Figure S1C



Supplementary Figure S2

PSD95

```

Human attttttttgggggaaaaaagggaagggaatgggtctatgggagtgagggaatgaggga----gggaaggga-
Chimp attttttttgggggaaaaaagggaagggaatgggtctatgggagtgagggaatgaggga----gggaaggga-
Rat attttttttgggggaaaaaagggaagggaatgggtctatgggagtgagggaatggga----gggaaggga-
Mouse attttttttgggggaaaaaagggaagggaatgggtctatgggagtgagggaatggga----gggaaggga-
Dog ttttttttgggggaaaagggaagggtgggtctatgggagtgaggga-gcgtggga----gggaaggga-
Opossum ttttttttgggggat--ggggaagggaagggaacagggggctggggtat--ggggattatgggaaggga-
  
```

PSD95

```

Human t-ggg----gggca--gggg-tcggggg-ggg-tgtccggggagccaggg
Chimp t-ggg----gggca--gggg-tcggggg-ggg-tgtccggggagccaggg
Rat tgggg----gggcaa-gggg-tcagggg-ggg-tgtccggggagccaggg
Mouse tgggg----gggcaa-gggg-tcagggg-ggg-tgtccggggagccaggg
Dog t-ggg----gggca--gggg-tcggggg-ggg-tgtcgtctggggagccaggg
Opossum tggggaga-gggaaaaagggg-----ggg-gggccttggggagc-tggg
  
```

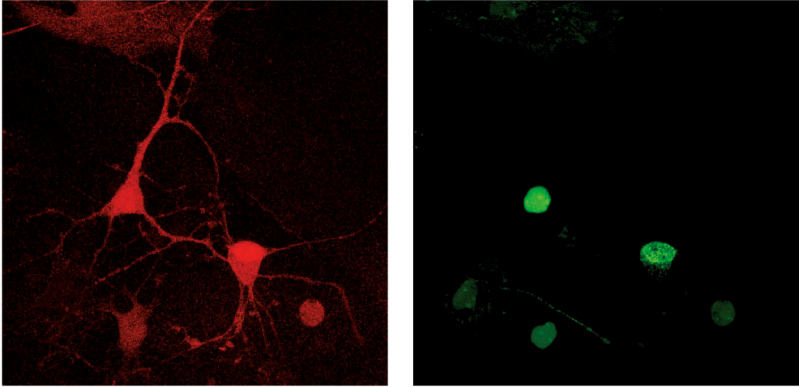
CaMKIIa

```

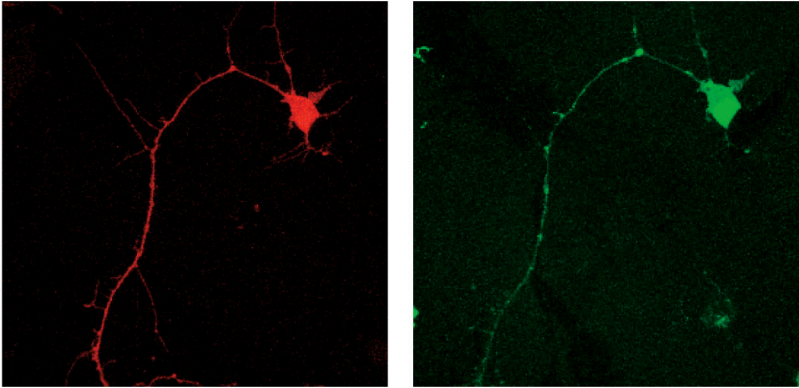
Human tttctgctattgaggggggcgggt--gggatgggaagaagggg-----catttgtttta
Chimp tttctgctatt---gggggggt--gggatgggaagaagggg-----cgtttgtttta
Rat tttctgctact----gggggggt--gggtg-ggg---gaggggagaagagacgtctgtttta
Mouse tttctgctact----gggggggt--ggg--gg---aggggagaagagatgtctggttta
Dog cttctgctact----gggagggga--ggg--gggaagaagggg-----tgtctgtttta
Opossum tttatgttgttt---ggtggggga--ggga--ggaagtgggg-----tgctgtctgtttta
  
```

Supplementary Figure S3

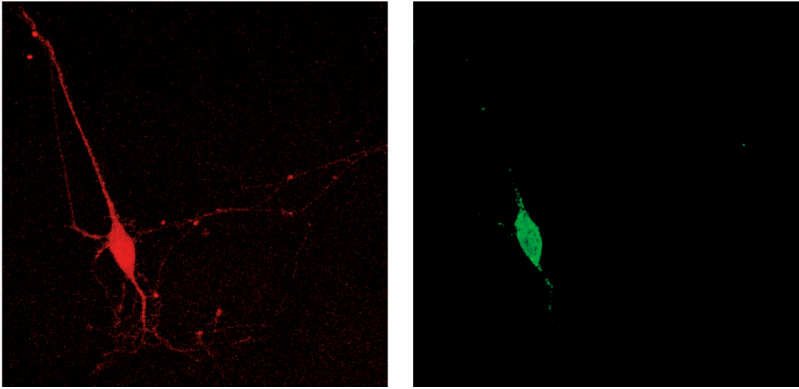
A BoxB-less



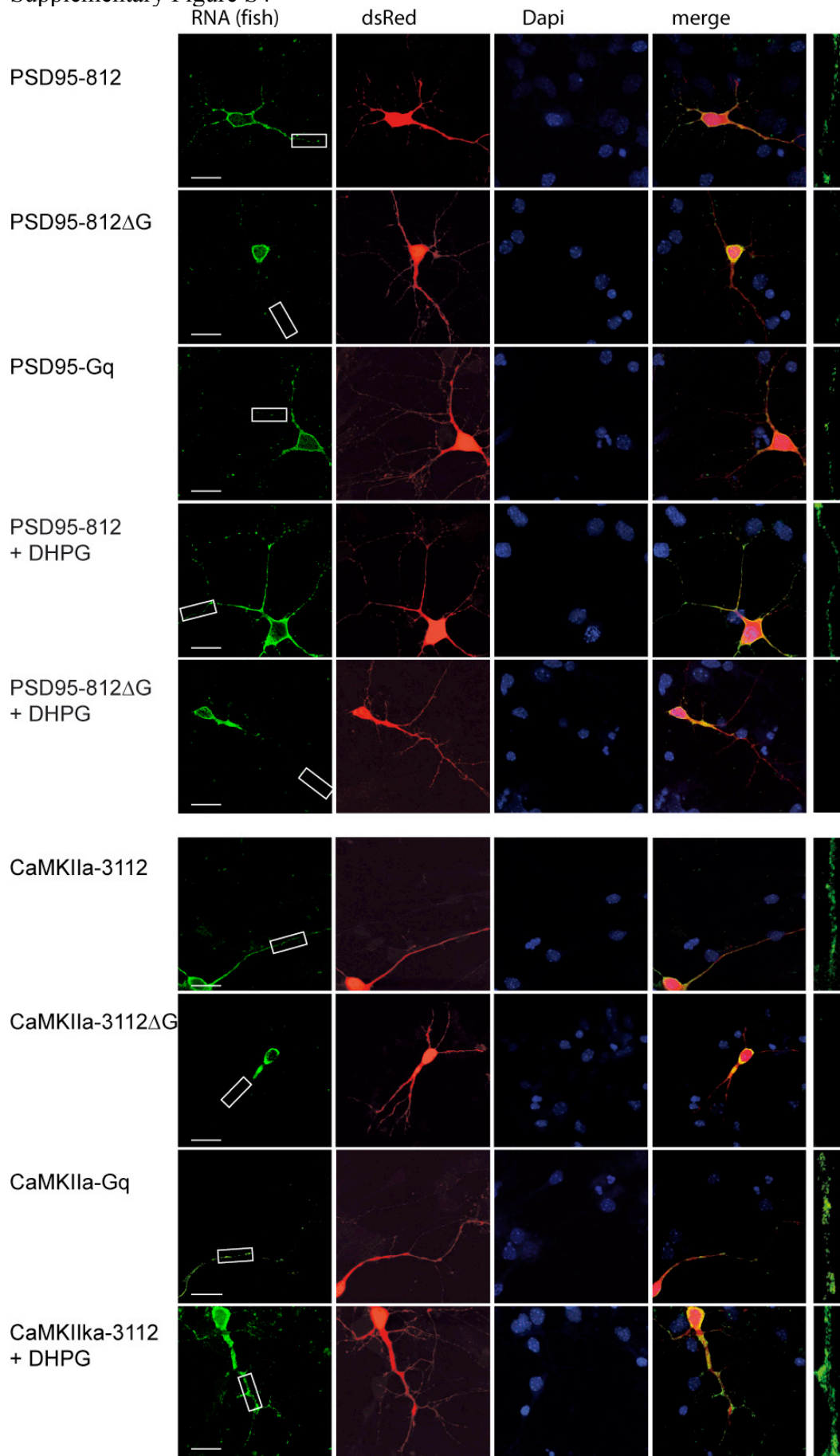
B BoxB +Zipcode



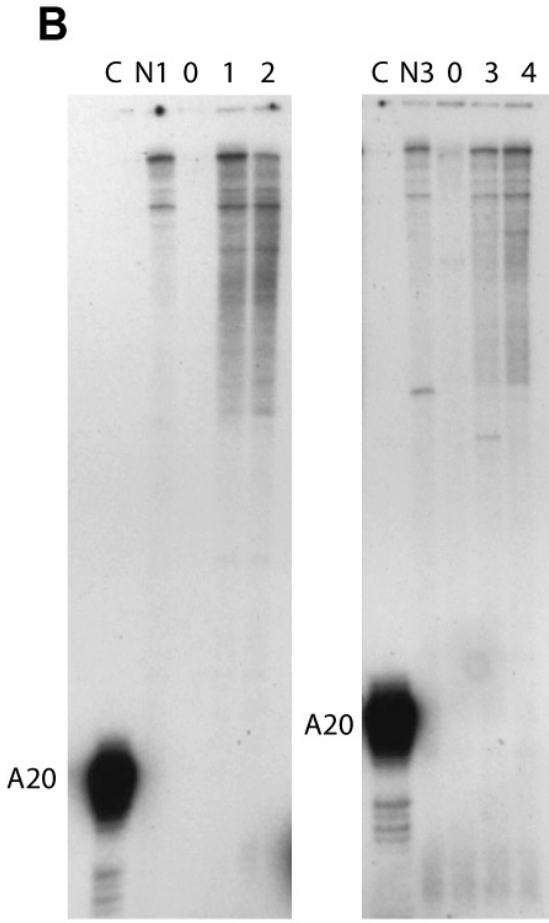
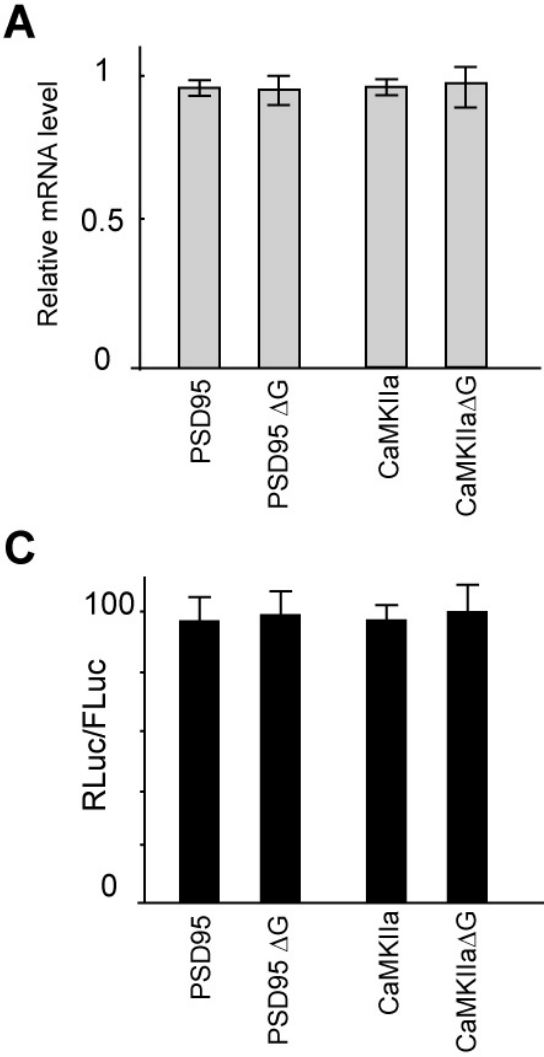
C BoxB



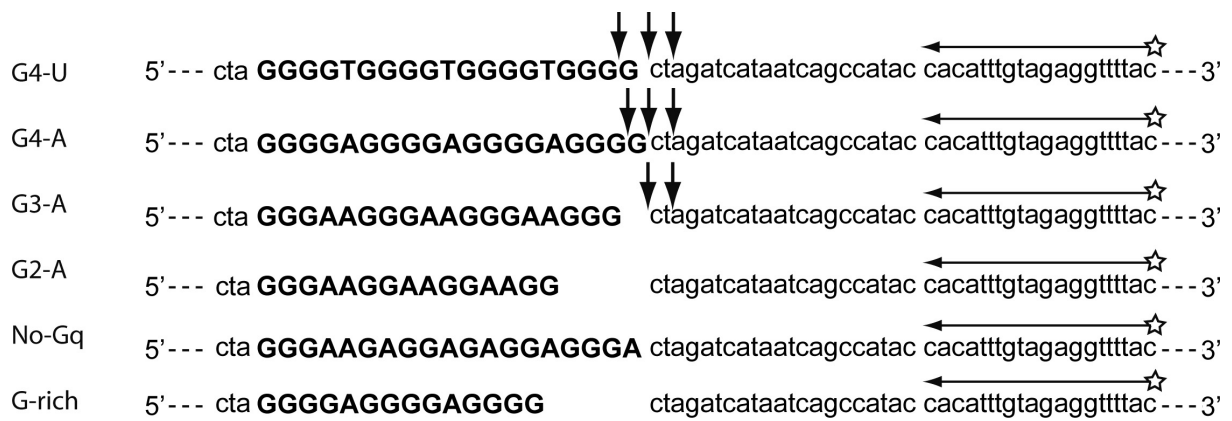
Supplementary Figure S4



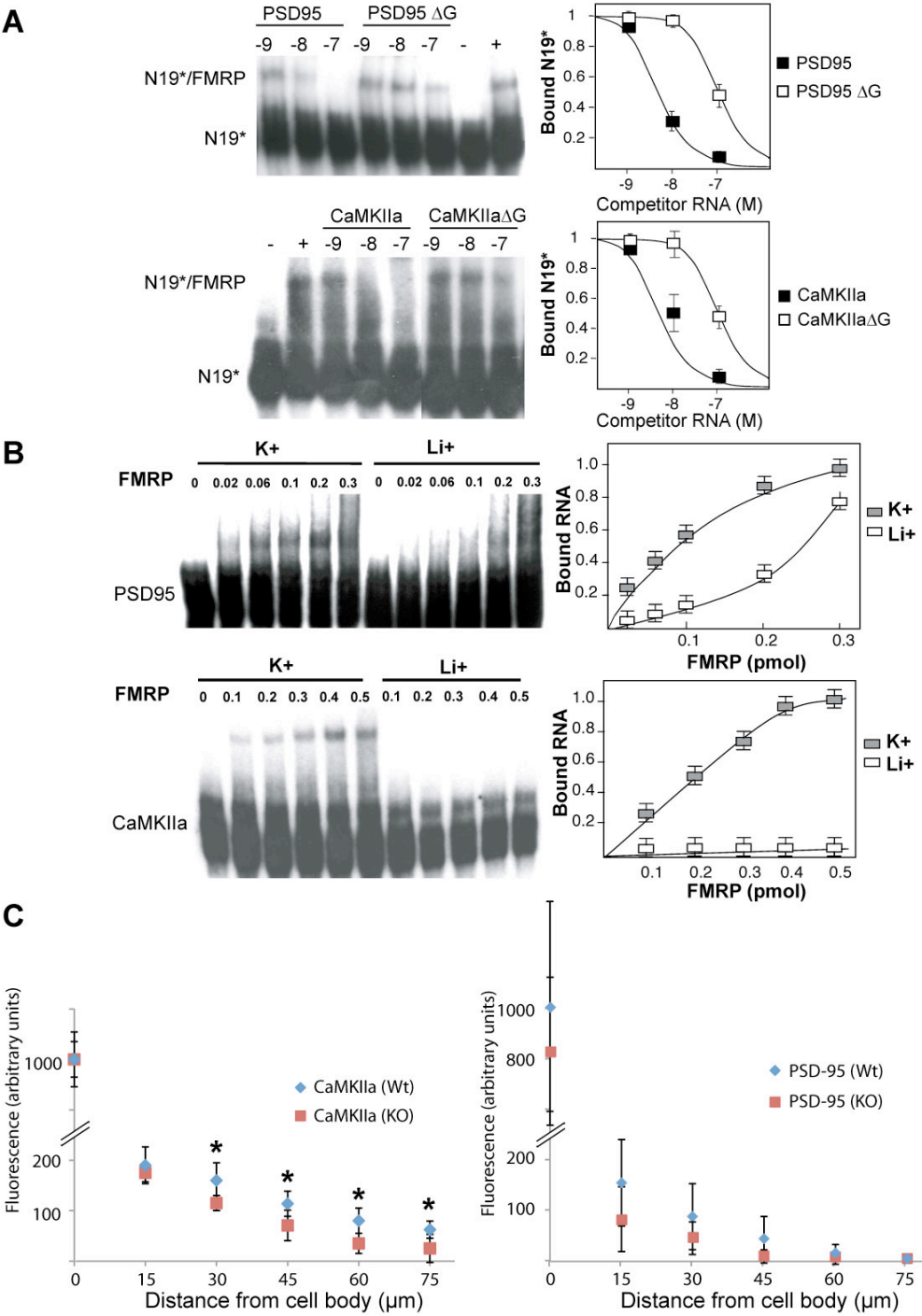
Supplementary Figure S5



Supplementary Figure S6



Supplementary Figure S7



Supplementary References

Daigle N, Ellenberg J (2007) LambdaN-GFP: an RNA reporter system for live-cell imaging. *Nat Methods* **4**(8): 633-636

Huang YS, Carson JH, Barbarese E, Richter JD (2003) Facilitation of dendritic mRNA transport by CPEB. *Genes Dev* **17**(5): 638-653

Kostadinov R, Malhotra N, Viotti M, Shine R, D'Antonio L, Bagga P (2006) GRSDB: a database of quadruplex forming G-rich sequences in alternatively processed mammalian pre-mRNA sequences. *Nucleic Acids Res* **34**(Database issue): D119-124

Moine H, Ehresmann B, Ehresmann C, Romby P (1998) Probing RNA structure and function in solution. In *RNA Structure and Function*, Simons RW, Grunberg-Manago M (eds), pp 77-115. Cold Spring Harbor Laboratory Press

Mori Y, Imaizumi K, Katayama T, Yoneda T, Tohyama M (2000) Two cis-acting elements in the 3' untranslated region of alpha-CaMKII regulate its dendritic targeting. *Nat Neurosci* **3**(11): 1079-1084

Murray EL, Schoenberg DR (2008) Assays for determining poly(A) tail length and the polarity of mRNA decay in mammalian cells. *Methods Enzymol* **448**: 483-504

Schaeffer C, Bardoni B, Mandel JL, Ehresmann B, Ehresmann C, Moine H (2001) The fragile X mental retardation protein binds specifically to its mRNA via a purine quartet motif. *Embo J* **20**(17): 4803-4813